



Original article

Targeting triple-negative breast cancer cells with 6,7-bis(hydroxymethyl)-1*H*,3*H*-pyrrolo[1,2-*c*]thiazoles

Kathleen Santos^a, Mafalda Laranjo^{a,b,c}, Ana Margarida Abrantes^{a,b,c}, Ana F. Brito^{a,c},
Cristina Gonçalves^{b,d}, Ana Bela Sarmiento Ribeiro^{b,d}, M. Filomena Botelho^{a,b,c},
Maria I.L. Soares^e, Andreia S.R. Oliveira^e, Teresa M.V.D. Pinho e Melo^{e,*}

^aBiophysics Unit, Faculty of Medicine of University of Coimbra, Azinhaga de Santa Comba, Celas, 3004-548 Coimbra, Portugal

^bCIMAGO – Center of Investigation in Environment, Genetics and Oncobiology, Faculty of Medicine of University of Coimbra, Azinhaga de Santa Comba, Celas, 3004-548 Coimbra, Portugal

^cIBILI – Institute for Biomedical Imaging and Life Science, Faculty of Medicine of University of Coimbra, Azinhaga de Santa Comba, Celas, 3004-548 Coimbra, Portugal

^dApplied Molecular Biology, University Clinic of Haematology, Faculty of Medicine of University of Coimbra, Coimbra, Portugal

^eDepartment of Chemistry, University of Coimbra, 3004-535 Coimbra, Portugal

ARTICLE INFO

Article history:

Received 1 February 2014

Received in revised form

1 April 2014

Accepted 4 April 2014

Available online 4 April 2014

Keywords:

6,7-Bis(hydroxymethyl)-1*H*,3*H*-pyrrolo[1,2-*c*]thiazole

Antitumor activity

Breast cancer

Triple-negative breast cancer

ABSTRACT

Further studies on 6,7-bis(hydroxymethyl)-1*H*,3*H*-pyrrolo[1,2-*c*]thiazoles as anticancer agents against breast cancer are reported, allowing to demonstrate the potential of these compounds for the therapy of the triple-negative breast cancer, the most challenging tumors in clinical practice. These compounds were assayed for their *in vitro* cytotoxicity on several human breast cancer cell lines (MCF7, HCC1954 and HCC1806 cell lines). Particularly interesting were the results obtained for 4-hydroxyphenyl substituted derivative, which proved to be the most promising compound regarding HCC1806 cell line, a triple-negative breast cancer. The effects of the two most active compounds on cell survival, viability, cell cycle, DNA damage and expression of proteins related to cell death pathways were studied. The reported results consolidate the potential of 6,7-bis(hydroxymethyl)-1*H*,3*H*-pyrrolo[1,2-*c*]thiazoles for the therapy of breast cancer, particularly the triple-negative.

© 2014 Elsevier Masson SAS. All rights reserved.

1. Introduction

Breast cancer is the most common cause of tumor malignancy in woman [1]. The breast cancer susceptibility genes (BRCA) 1 and 2 are the most associated with breast cancer. BRCA 1 gene is important in the normal breast development promoting the expression of estrogen receptors (ER) and BRCA2 gene is responsible for the mechanism of DNA repair by homologous recombination (HR). Mutations in BRCA genes result in a more aggressive and metastatic phenotype, usually referred as *BRCAness* phenotypes. However, these are the types of cancer more susceptible to chemotherapy due to their compromised DNA repair mechanism [2]. Even triple-negative breast cancers (TN – which have negative histochemical confirmation for ER, progesterone receptor, RP, and human epidermal growth factor receptor 2, HER2), without mutations in

BRCA genes have also been described as having a *BRCAness* phenotype and are as sensitive to chemotherapy [3].

The triple-negative breast cancer is an extremely aggressive form of breast cancer that occurs most often in young women. It is difficult to treat successfully because there are no targeted therapies available as it lacks the receptors usually used for clinical stratification. Triple-negative breast cancers tend to present higher grades, larger tumors, higher metastasis incidence and a shorter time of recurrence compared with other breast cancers types. The lack of adequate therapeutic response for TN breast cancers makes the search for new anti-cancer agents extremely relevant. Thus, we were particularly interested in finding compounds with anti-triple-negative breast cancer properties.

In recent years we have studied chiral hydroxymethyl-1*H*,3*H*-pyrrolo[1,2-*c*]thiazoles as promising antiproliferating agents against breast cancer [4,5], leading to the synthesis of chiral 6,7-bis(hydroxymethyl)-1*H*,3*H*-pyrrolo[1,2-*c*]thiazoles as the most promising scaffold for the design of new potent anticancer compounds against breast cancer.

* Corresponding author.

E-mail address: tmelo@ci.uc.pt (T.M.V.D. Pinho e Melo).

Structure–activity relationship (SAR) studies of several 1*H*,3*H*-pyrrolo[1,2-*c*]thiazole derivatives (e.g. **1–6**) against breast adenocarcinoma MCF7 cell line allowed the establishment of structural features for antitumor activity, Fig. 1 [4,5]. It was demonstrated that only 1*H*,3*H*-pyrrolo[1,2-*c*]thiazoles bearing hydroxymethyl substituents show *in vitro* anticancer activity. On the other hand, the position of the hydroxymethyl substituent is crucial. In fact, derivative **1** with this group at C-6 is active whereas the C-7 substituted derivative **2** showed low activity. Nevertheless, the presence of two hydroxymethyl groups leads to a slight improvement in activity against MCF7 breast cancer cell lines as illustrated by 6,7-bis(hydroxymethyl)-1*H*,3*H*-pyrrolo[1,2-*c*]thiazole **3** with IC₅₀ value of 1.1 μM. Furthermore, the combined presence of a phenyl group at C-3 and a methyl group at C-5 in the 1*H*,3*H*-pyrrolo[1,2-*c*]thiazole ring system is essential to ensure high cytotoxicity. Interestingly, pyrrolo[1,2-*c*]thiazole **6** showed even better performance against breast cancer cell lines than the corresponding enantiomer **3**.

In an effort to produce new structures with better anticancer activity and that may give additional knowledge on SAR, based on structure **3**, we synthesized and evaluated the effect of replacing the phenyl substituent at C-3 by a 4-methoxyphenyl group **9a** and by the more hydrophilic 4-hydroxyphenyl group **9b**. The 6,7-bis(hydroxymethyl)-1*H*,3*H*-pyrrolo[1,2-*c*]thiazole **12**, derived from penicillamine, has also been studied in order to determine whether the presence of two methyl groups at C-1 would lead to enhance cytotoxic activity. The new compounds were assayed for their *in vitro* cytotoxicity on several human breast cancer cell lines, including TN breast cancer cell lines.

So far our studies were limited to cytotoxicity of the compounds synthesized. However, to understand the mechanism of action and the effects on cancer biology further studies were needed. Therefore, we evaluated the effects of two promising compounds on cell survival, viability, cell cycle, DNA damage and expression of proteins related to cell death pathways.

2. Results and discussion

2.1. Chemistry

Chiral 6,7-bis(hydroxymethyl)-1*H*,3*H*-pyrrolo[1,2-*c*]thiazoles **9a** and **9b** were prepared as outlined in Scheme 1, following a known general synthetic procedure [4]. 2-Phenylthiazolidine-4-carboxylic acids **7** were obtained as a mixture of 2*R*,4*R*- and 2*S*,4*R*-diastereoisomers from the reaction of L-cysteine with the appropriate aldehyde. Thiazolidines **7** were heated in a solution of acetic anhydride in the presence of dimethyl acetylenedicarboxylate. Under

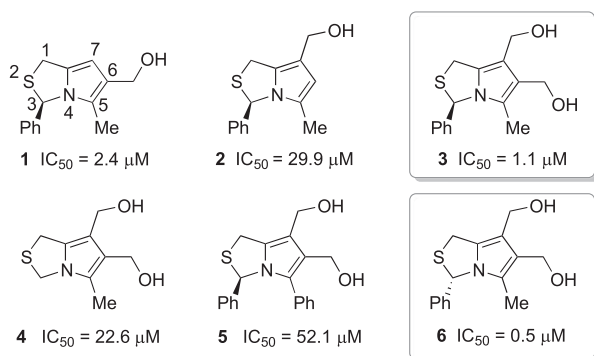
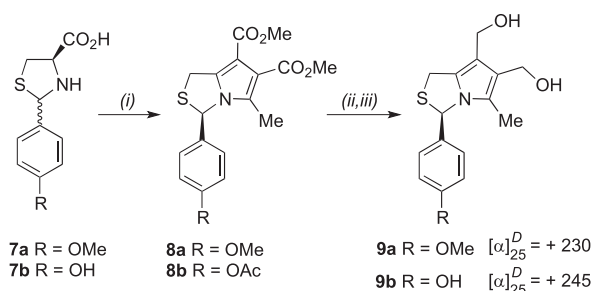


Fig. 1. Cytotoxicity against MCF7 breast cancer human cell line (72 h incubation time) [4,5].



Scheme 1. Synthesis of 1*H*,3*H*-pyrrolo[1,2-*c*]thiazoles **9**. Reagents and conditions: (i) Ac₂O, DMAD, reflux, 4 h; (ii) DCM, LiAlH₄ in diethyl ether, 0 °C; (iii) reflux, 1.5 h; **9a**: 58%, **9b**: 52%.

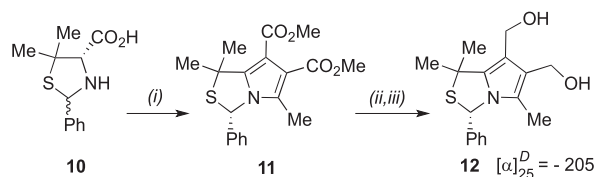
these reaction conditions the *N*-acylation of thiazolidines occurs *in situ*, followed by 1,3-dipolar cycloaddition via a bicyclic münchnone intermediate. The chirality at C-4 of the starting thiazolidine is lost and the chirality at C-2 (C-3 in the product) is retained giving 1*H*,3*H*-pyrrolo[1,2-*c*]thiazole-6,7-dicarboxylates **8** as single enantiomers with *R* configuration at C-3. The cycloaddition of the münchnone generated from thiazolidine **7b** gave 3-(4-acethoxyphenyl)-1*H*,3*H*-pyrrolo[1,2-*c*]thiazole **8b**, resulting from the acetylation of the initially formed dimethyl (3*R*)-3-(4-hydroxyphenyl)-5-methyl-1*H*,3*H*-pyrrolo[1,2-*c*]thiazole-6,7-dicarboxylate. Reduction of 1*H*,3*H*-pyrrolo[1,2-*c*]thiazoles **8** with lithium aluminum hydride afforded the corresponding 6,7-bis(hydroxymethyl)-1*H*,3*H*-pyrrolo[1,2-*c*]thiazoles **9** in moderate yield. In the case of acetylated derivative **8b** simultaneous deprotection of the hydroxyl group has occurred giving compound **9b**.

A similar synthetic strategy was applied in the synthesis of (3*S*)-3-phenyl-1,1,5-trimethyl-6,7-bis(hydroxymethyl)-1*H*,3*H*-pyrrolo[1,2-*c*]thiazole (**12**) (Scheme 2). 5,5-Dimethyl-2-phenylthiazolidine-4-carboxylic acid (**10**) was prepared as a mixture of 2*R*,4*S*- and 2*S*,4*S*-diastereoisomers from the reaction of D-penicillamine with benzaldehyde. The 1,3-dipolar cycloaddition of the münchnone, generated from thiazolidine **10**, gave 1*H*,3*H*-pyrrolo[1,2-*c*]thiazole-6,7-dicarboxylate **11** as a single enantiomer with *S* configuration. 6,7-Bis(hydroxymethyl)-1*H*,3*H*-pyrrolo[1,2-*c*]thiazole **12** was obtained in 51% yield by the reduction of compound **11** with lithium aluminum hydride.

2.2. Biological evaluation

2.2.1. In vitro antiproliferative activities and SAR

The new compounds were evaluated for their *in vitro* antiproliferative activity against human breast cancer representative of HER2⁺ (HCC1954), RH⁺ (MCF7) and TN (HCC1806) tumors (Table 1). In the HCC1954 cell line none of the compounds affect cell proliferation at 24 h of incubation. However, when cells were incubated for 48 h with the studied compounds a significant decrease in IC₅₀ values was observed (**3**, **9a** and **9b** *p* < 0.001; **6** *p* = 0.019; **12** *p* = 0.017). **3** is the most promising anti-proliferative



Scheme 2. Synthesis of 1*H*,3*H*-pyrrolo[1,2-*c*]thiazole **12**. Reagents and conditions: (i) Ac₂O, DMAD, reflux, 4 h; (ii) DCM, LiAlH₄ in diethyl ether, 0 °C; (iii) reflux, 1.5 h; **12**: 51%.

Table 1

IC₅₀ values of the compounds **3**, **6**, **9** and **12** for 24, 48, 72 and 96 h of incubation in the MCF7, HCC1954 and HCC1806 cell lines.^a

Compd	Incubation time	IC ₅₀ (μM) ^b		
		HCC1806	HCC1954	MCF7
3	24 h	>100	98.2	12.2 ⁵
	48 h	81.4	27.0	1.9 ⁵
	72 h	51.3	26.2	1.0 ⁵
	96 h	13.9	24.9	0.6 ⁵
6	24 h	>100	>100	1.75 ⁵
	48 h	63.1	56.8	0.54 ⁵
	72 h	78.5	14.8	0.54 ⁵
	96 h	28.7	11.8	0.30 ⁵
9a	24 h	89.0	>100	>100
	48 h	28.0	84.4	46.9
	72 h	19.4	56.1	32.7
	96 h	12.3	19.2	6.6
9b	24 h	80.3	>100	>100
	48 h	26.4	65.6	86.2
	72 h	11.9	46.6	53.9
	96 h	5.4	27.4	29.5
12	24 h	>100	99.5	>100
	48 h	41.7	69.0	>100
	72 h	26.9	55.9	>100
	96 h	21.3	33.5	>100

^a Cells were incubated with DMSO solutions of the selected compounds, washed and then cell proliferation was evaluated by MTT test.

^b Concentration needed to inhibit cell proliferation by 50% as determined from dose–response curves by exponential decay fitting ($r^2 > 0.9$).

compound against HCC1954 cells and the less promising is **9a**. In the MCF7 cell line, **3** and **6** are the most promising compounds concerning anti-proliferative activity with IC₅₀ values of 0.6 μM and 0.3 μM, respectively, for 96 h incubation time. On the other hand, **12** showed no anti-proliferative activity against MCF7 cell line, in the concentrations tested, up to 100 μM. Despite the fact that **9a** and **9b** showed moderate anti-proliferative activity in MCF7 cell line, the decreasing IC₅₀ value over time has statistical significance ($p < 0.05$). In the HCC1806 cell line, **9b** is the most promising compound with significant decrease of IC₅₀ value over time ($p < 0.05$), with IC₅₀ value of 5.4 μM for 96 h incubation time. All the other compounds showed a significant decrease in the IC₅₀ value going from 24 h to 48 h incubation time ($p < 0.001$), being **3** and **6** the less active compounds in this cell line.

The design of new compounds has been guided considering **3** as the lead compound [5] and the structural modifications were thought not only to obtain derivatives with higher anti-proliferation activity, but also to gather data regarding SAR. We showed that the presence of the phenyl group at C-3 seemed to be important to the activity of the compounds [5]. However, in previous studies, the possibility of replacing the phenyl group by other aryl groups such as 4-methoxyphenyl and 4-hydroxyphenyl substituents was not explored. In this context, we synthesized 3-(4-methoxyphenyl)-1*H*,3*H*-pyrrolo[1,2-*c*]thiazole **9a** and 3-(4-hydroxyphenyl)-1*H*,3*H*-pyrrolo[1,2-*c*]thiazole **9b**. Regarding MCF7 cell line the new derivatives show lower activity than the lead compound **3**. However, these compounds presented better anticancer activity than 1*H*,3*H*-pyrrolo[1,2-*c*]thiazole **3**, against TN cell line, HCC1806, which is more challenging to treat and lack a targeted therapy. Particularly interesting were the results obtained for 4-hydroxyphenyl substituted derivative **9b**, which prove to be the most promising compound regarding HCC1806 cell line, a TN-breast cancer.

So far, all the compounds studied in our group were unsubstituted at C-1. Thus, 1,1-dimethyl-1*H*,3*H*-pyrrolo[1,2-*c*]thiazole **12** was synthesized and its biological evaluation as anticancer activity against HCC1806, HCC1954 and MCF7 breast cancer human cell

lines was carried out (Table 1). However, the IC₅₀ values obtained for **12** were rather high in comparison with other studied compounds. Thus, from current and previous results, we can conclude that substitution at C-1 by methyl groups does not improve anticancer activity of 1*H*,3*H*-pyrrolo[1,2-*c*]thiazole derivatives. Moreover, **12** has the *S* absolute configuration at C-3, which potentiates cytotoxic activity against MCF7 cell line, as we already discussed. These results indicate that the substitution pattern in the pyrrolo [1,2-*c*]thiazole ring system plays a more significant role in the anti-proliferative activity than the absolute configuration at C-3.

2.2.2. Cell cultures are sensitive to treatment

Since 1*H*,3*H*-pyrrolo[1,2-*c*]thiazoles **3** and **9b** are promising due to their anti-proliferative activity against HR⁺ MCF7 cell line and TN HCC1806 cell lines, we tested the long-term sensitivity and survival of a cell culture to the treatment performing the clonogenic assay. As we can observe in Fig. 2, all treatments reduces significantly ($p < 0.001$) the surviving factor of both cell cultures. It is further noticed that HCC1806 cell line is particularly sensitive to treatment since surviving factor is below 2%.

These results show that HCC1806 cell line in particular presents high sensitivity to chemotherapy with these compounds, proving that this cell line presents a *BRCAness* phenotype. It is further noticed that treatment with **3**, which is the compound that presents the higher IC₅₀ value, is the one that most affects HCC1806 survival.

2.2.3. Cell mass and total protein production is reduced

The total protein content was analyzed after treatment of MCF7 and HCC1806 cell lines with 1*H*,3*H*-pyrrolo[1,2-*c*]thiazoles **3** and **9b** (Fig. 3). HCC1806 cell line reduces the total protein content to about 50% when treated with any of the compounds. In the MCF7 cell line, treatment with **3** produces similar results to those of HCC1806 cell line, but treatment with **9b** reduces total protein content to $15.4 \pm 9.4\%$. The reduction of protein content showed statistical significance in all conditions of treatment in both cell lines ($p < 0.001$). SRB assay allows us to conclude that cell mass is significantly reduced with treatment, which indicates that cell viability is also significantly reduced.

2.2.4. PT induce cell death preferentially by late apoptosis and necrosis

In view of the high cytotoxicity exhibited against MCF7 and HCC1806 by 1*H*,3*H*-pyrrolo[1,2-*c*]thiazoles **3** and **9b** and SRB assay results which indicates a reduced viable cell mass, flow cytometry studies were performed with IC₅₀ values of these compounds at 48 h to determine cell viability and the induced mechanism of cell death (necrosis or apoptosis). The graphs showed in Fig. 4 presents the percentage and standard deviation for populations of four different cell states: living cells (negative for An-V and PI), apoptotic cells (negative for PI and positive for An-V), late apoptotic or necrotic cells (positive for An-V and PI) and necrotic cells (negative for An-V and positive for PI).

For the MCF7 cell line it is observed that **3** induces a decreasing in the viable cells population ($p = 0.015$) and an increasing in the late apoptotic/necrotic ($p = 0.048$) and in the necrotic populations ($p = 0.001$). **9b** effects in MCF7 cell line decreased viable cells population to $21.4 \pm 4.2\%$ ($p < 0.001$), and increased apoptotic ($p = 0.001$), late apoptotic/necrotic ($p < 0.001$) and necrotic ($p = 0.006$) populations, comparing to the control.

In the TN cell line, HCC1806, both **3** and **9b** decreases viable cells population (**3**: $p < 0.001$; **9b**: $p = 0.022$) and increases late apoptosis/necrosis (**3**: $p < 0.001$; **9b**: $p = 0.011$) and necrosis (**3**: $p < 0.001$; **9b**: $p = 0.019$). HCC1806 cell line is characterized by a 2bp insertion after the nucleotide 256 in the 4th exon in 17p13.1

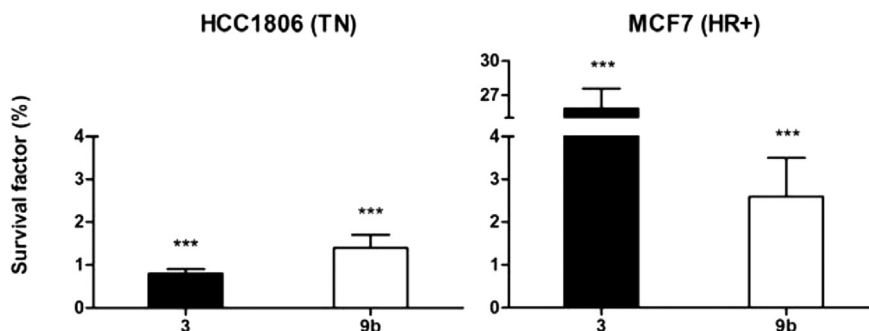


Fig. 2. Survival factor of MCF7 and HCC1806 cell lines incubated with **3** and **9b** during 48 h. Results are presented as mean \pm SD ($n \geq 8$). The * represent significant differences between the respective control population. Statistical significance: *** $p < 0.001$.

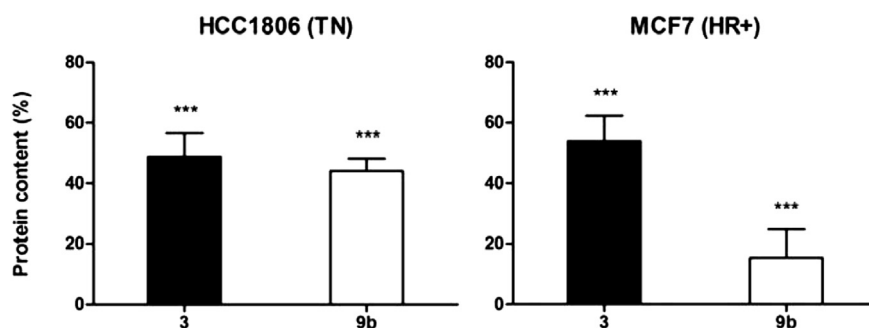


Fig. 3. Protein content of MCF7 and HCC1806 cell lines incubated with **3** and **9b** during 48 h. Results are presented as mean \pm SD ($n \geq 8$). The * represent significant differences between the respective control population. Statistical significance: *** $p < 0.001$.

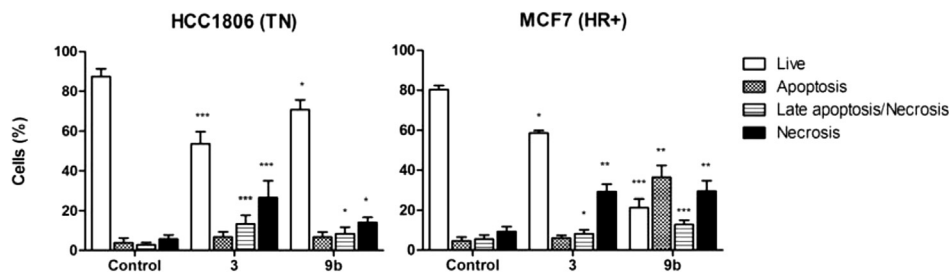


Fig. 4. Cell viability of MCF7 and HCC1806 cell lines incubated with **3** and **9b** during 48 h. Cell viability results represent the percentage of viable cells, cells in apoptosis, cells in late apoptosis/necrosis and cells in necrosis and are presented as mean \pm SD ($n \geq 5$). The * represent significant differences between the respective control population. Statistical significance: * $p < 0.05$; ** $p < 0.01$; *** $p < 0.001$.

chromosome [6], which encodes p53, causing a frame shift which results in a shorter protein with only 122 aminoacids. Therefore HCC1806 lacks p53 expression⁷ due to the degradation of a non-functional p53 protein and, as consequence, cellular death by apoptosis is diminished. That is the reason why p53 loss is correlated with multidrug resistance and also with defective cell proliferation control, inefficient DNA repair and genetic instability and that contributes to the aggressive phenotype due to cumulative genetic alteration [7].

On the other hand, MCF7 cell line expresses the wild-type p53 [7], which could explain the duality of response to treatment in the clonogenic assay and viability and types of cell death. That is, cell viability is reduced to about 55/60% when both cell lines are treated with **3** and also late apoptotic/necrotic and necrotic populations are significantly increased which means that the response to treatment is probably p53 independent. However, when cells are treated with **9b** their response is very distinct. MCF7 viability is significantly reduced to $21.4 \pm 4.2\%$ and the apoptotic population is significantly

increased, although with time cells are able to recover as observed with the clonogenic assay, which means that, initially the majority of cells are affected and die but the remaining cells are able to recover after treatment. On the other hand HCC1806 is more resistant to cell death and clearly cell death through apoptosis is compromised since cell death is mainly necrotic with both treatments but its long-term survival is significantly reduced to $1.4 \pm 0.3\%$.

2.2.5. p53 expression is influenced by 1H,3H-pyrrolo[1,2-c]thiazole **3**

Although the p53 profile of the two cell lines is known, we confirmed that the HCC1806 cell line lacks its expression. Nevertheless we evaluated p53 expression by western blot to access this protein in the MCF7 cell line in response to treatment.

As we can observe in Fig. 5, p53 is increased with treatment in the MCF7 cell line, with a significant effect with **9b** treatment ($p < 0.009$). This result corroborates the increasing of the apoptotic

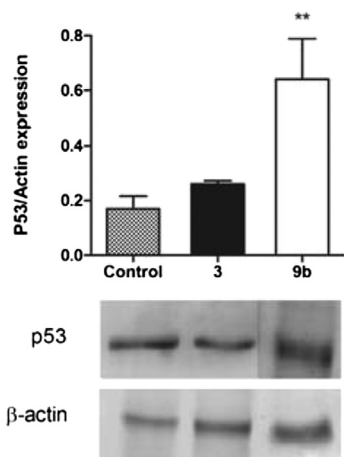


Fig. 5. p53 Protein expression. The graphic represents ratio of p53 expression versus β -actin and the image refers to a representative immunoblot of p53 and β -actin. Results are presented as mean \pm SD ($n \geq 3$). The * represent significant differences between the respective control population. Statistical significance: ** $p < 0.01$.

population after **9b** treatment, and the slight non significant increase of p53 expression compared to control, after **3** treatment, explains why cell death is not related to apoptosis.

2.2.6. 1*H*,3*H*-pyrrolo[1,2-*c*]thiazole increases Bax/Bcl-2 ratio

We also assessed the ratio of the expression of Bax, a pro-apoptotic protein, and Bcl-2, an anti-apoptotic protein, two proteins involved in the apoptotic cell death (Fig. 6). Briefly, this pathway is mainly activated in response to DNA damage, which can activate p53 resulting in the expression of Bax and repression of Bcl-2 proteins. Later, Bax leads to the cytochrome *c* release from mitochondria and later caspase activation, ultimately causing cell death by apoptosis [7,8].

Comparing to the control, the ratio Bax/Bcl-2 is increased in all treatments, however only treatment with **9b** increase this ratio with statistical significance (MCF7: $p = 0.003$; HCC1806: $p < 0.001$). As we can observe Bax/Bcl-2 ratio in the MCF7 cell line is consistent with results of cell death and p53 expression, where only treatment with **9b** was able to induce a significant increase in the apoptotic cell population.

Despite the fact that HCC1806 cell line does not express p53, the Bax/Bcl-2 ratio is significantly increased with **9b** treatment. This might have to do with the default Bax activation when anti-apoptotic proteins such as Bcl-2 are neutralized or their expression is diminished [9]. However cell death is mainly necrotic, which means that other mechanisms of cell death might be predominant.

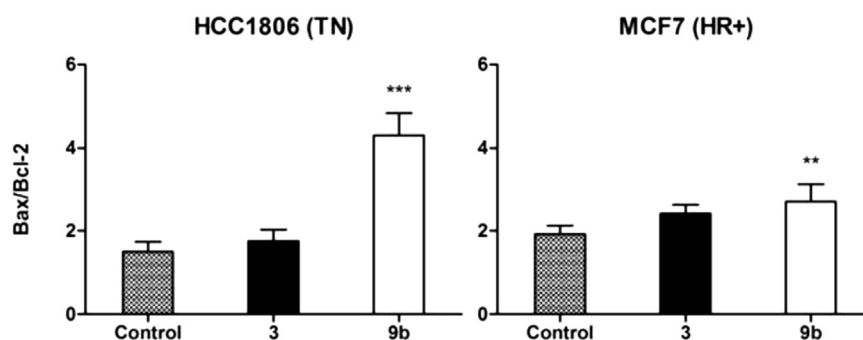


Fig. 6. Ratio of the mean fluorescence intensity of Bax and the mean fluorescence intensity of Bcl2 in MCF7 and HCC1806 cell lines incubated with **3** and **9b** during 48 h. Results are presented as mean \pm SD ($n \geq 5$). The * represent significant differences between the respective control population. Statistical significance: ** $p < 0.01$; *** $p < 0.001$.

For instance, poly(ADP-ribose)polymerase-1 (PARP-1) promotes cell death by apoptosis when DNA damage is moderate and cell death by necrosis in the presence of extensive DNA damage, but also the balance between apoptosis and necrosis is dependent of the cell type [10]. With that in mind 1*H*,3*H*-pyrrolo[1,2-*c*]thiazole **3** could cause severe DNA damage and activate PARP-1 causing necrotic cell death, and also HCC1806 cell line could be more sensitive to the activation of this protein since both treatments cause necrotic cell death.

2.2.7. 1*H*,3*H*-pyrrolo[1,2-*c*]thiazole blocks cell-cycle progression preferentially at S phase

The growing evidence that these compounds could induce DNA damage led to the analysis the progress/blockade of cell cycle of MCF7 and HCC1806 cell lines after treatment with **3** and **9b**. In the MCF7 cell line, both **3** and **9b**, as represented in Fig. 7, decreased population of cells in the G0/G1 (**3** and **9b**: $p < 0.001$) and increased cell population in the S phase (**3** and **9b**: $p < 0.001$). A blockade in the G₂/M phases is induced by compound **3** ($p = 0.001$) but not by **9b** ($p > 0.05$). Both intra-S [11] and the G₂/M [12] checkpoints are mostly related to stalled replication forks that can derived from DNA inter-strand crosslinks. When this particular type of DNA damage is detected, ataxia telangiectasia and Rad3 related (ATR) is activated and promotes mainly checkpoint protein kinase 1 (Chk1) phosphorylation [12], a protein responsible for the intra-S phase arrest in order to promote DNA repair [11]. Also, Chk1-P is able to activate p53 protein, upregulating p21^{WAF1} which inhibit the cyclin-dependent kinase 1-cyclin B complex (Cdk1-cyclin B) and cause cell cycle G₂/M phase arrest [12].

As can be observed in Fig. 7, **3** induces a blockade in the G0/G1 phase in HCC1806 cell line ($p = 0.001$), but has no effect in the other phases of the cell cycle, indicating a state of quiescence where cells stop dividing [13]. Similarly to treatment in the MCF7 cell line, **9b** produced a decreased population of HCC1806 cells in the G0/G1 ($p < 0.001$) and an accentuated accumulation of cells in the S phase ($p < 0.001$) and in the pre-G0 phase ($p = 0.011$). These results indicate DNA degradation and intra-S phase arrest with the objective to promote DNA repair [11] as previously explained.

2.2.8. Comet assay in the MCF7 and HCC1806 cell lines

Because of the chemical structure of the compounds it was proposed that they could be able to act by mono and bis-alkylation of DNA. The alkaline comet assay (pH > 13) allows to detect DNA damage in individual eukaryotic cells, namely, single strand breaks, double strand breaks, alkaline labile sites, and transient repair sites [14]. As can be observed in Fig. 8, cells treated with IC₅₀ and with three times more this concentration do not show evidence of DNA breaks, in contrast with the positive controls with hydrogen

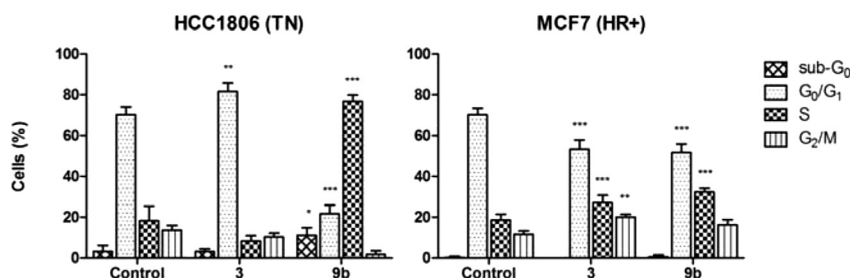


Fig. 7. Cell cycle analysis of MCF7 and HCC1806 cell lines incubated with **3** and **9b** during 48 h. Cell cycle results show the percentage of cell populations in the sub-G₀, G₀/G₁, S and G₂/M phases. Results are presented as mean \pm SD ($n \geq 5$). The * represent significant differences between the respective control population. Statistical significance: * $p < 0.05$; ** $p < 0.01$; *** $p < 0.001$.

peroxide. In fact, cells from treatment have the same appearance as the negative controls. However, we cannot exclude the possibility of intrastranded or interstranded crosslinking formation. Inter-stranded crosslinking is also a cytotoxic form of DNA damage once DNA strands separation is prevented and DNA replication is blocked. Concerning comet assay the presence of crosslinks results in less DNA migration [15].

3. Conclusion

Herein, in the continuation of our series of studies on the hydroxymethyl-1*H*,3*H*-pyrrolo[1,2-*c*]thiazoles as anticancer agents

against breast cancer, we introduce the potential of these compounds also for the triple-negative breast cancer, the most challenging tumors in clinical practice.

The study allowed us to redraw some conclusions regarding structure–activity relationships. Thus, the results of the *in vitro* activity have demonstrated that the presence of methyl groups at C-1 in the 1*H*,3*H*-pyrrolo[1,2-*c*]thiazole ring system is prejudicial for their activity, in all cell lines studied. The presence of a hydroxyphenyl group at C-3 seems to improve the anti-cancer activity for the TN cell line. These results, together with our previous ones, indicate that there is a differential anti-cancer activity concerning the biochemical profile of the cell lines, therefore future modifications must be envisioned taking this into account.

Furthermore, it is the first time that cellular effects beyond cytotoxicity are explored adding a new and valuable role in the screening of our compounds, giving a first insight into their mechanism of action. Both cell lines are sensitive to **3** and **9b** being the TN cell line HCC1806 survival the most affected/reduced. Viability is also decreased and cell death related proteins p53, Bax and Bcl-2 are significantly altered, occurring cell cycle blockage mainly in S-phase and cell death mostly by late apoptosis and necrosis. The reported results indicate that the studied compounds may induce DNA damage.

Our studies in this family of compounds consolidate the potential of hydroxymethyl-1*H*,3*H*-pyrrolo[1,2-*c*]thiazoles for the therapy of breast cancer, particularly the triple-negative, an asset to continue with pre-clinic studies.

4. Experimental section

4.1. Synthetic procedures

4.1.1. General methods

¹H NMR (400 MHz) and ¹³C NMR (100 MHz) spectra were recorded on a Bruker Avance III 400 MHz spectrometer. Chemical shifts (δ) are expressed in parts per million (ppm) related to internal TMS, and coupling constants (*J*) are in hertz. The following abbreviations are used in the assignment of NMR signals: s (singlet), d (doublet), m (multiplet), bs (broad singlet). IR spectra were recorded on a Nicolet 6700 FTIR spectrometer. HRMS spectra were obtained on a VG Autospect M spectrometer (TOF MS EI+ or ESI). Melting points were determined in open glass capillary with an Electrothermal melting point apparatus and are uncorrected. Optical rotations were measured on an Optical Activity AA-5 electrical polarimeter. Flash column chromatography was performed with silica gel 60 as the stationary phase. TLC analyses were carried out on Merck Silica gel 60 F254 plates. 1*H*,3*H*-Pyrrolo [1,2-*c*]thiazoles **3** [4] and **6** [5] were prepared as described in the literature.

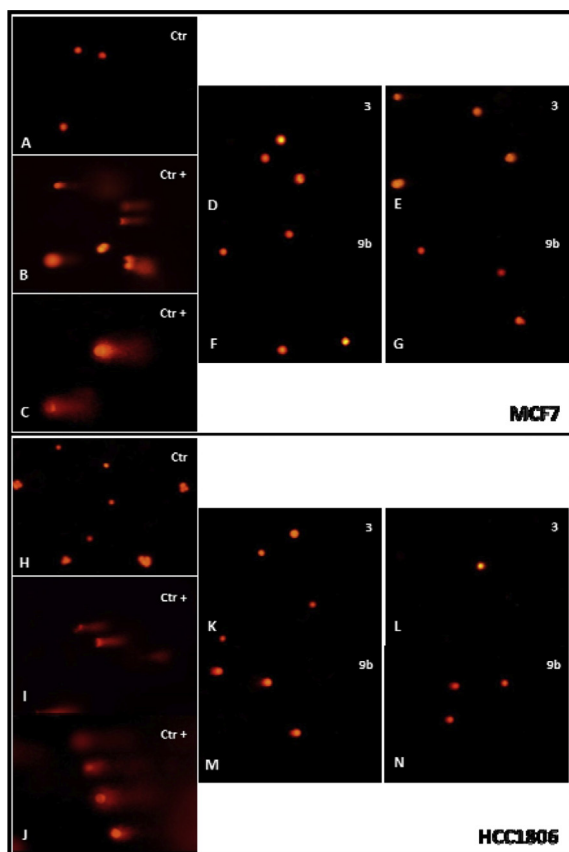


Fig. 8. Representative images of the Comet Assay in the MCF7 and HCC1806 cell lines after 48 h of incubation with **3** and **9b** in the concentrations equal to the IC₅₀ and three times this value. A and H: Control, untreated cell cultures, 100 \times ; B and I: positive control, 100 \times ; C and J: positive control, 400 \times ; D and K: **3** IC₅₀ treated cultures, 100 \times ; E and L: **3** 3 \times IC₅₀ treated cultures, 100 \times ; F and M: **9b** IC₅₀ treated cultures, 100 \times ; G and N: **9b** 3 \times IC₅₀ treated cultures, 100 \times .

4.1.2. General procedure for the synthesis of 1,3-thiazolidine-4-carboxylic acids **7**

A solution of the appropriate aldehyde (40.0 mmol) in ethanol (30 mL) was added to a solution of L-cysteine (5.0 g, 40.0 mmol) in water (40 mL). After stirring overnight at room temperature the product was filtered and washed with diethyl ether.

4.1.2.1. 2-(4-Methoxyphenyl)-1,3-thiazolidine-4-carboxylic acid (7a). Yield: 89% (8.5 g), white solid, mp 166–168 °C (lit. [16] 156–158 °C). The ¹H NMR spectrum obtained at 40 °C showed the presence of the two diastereoisomers (2*R*,4*R*) and (2*S*,4*R*) (ratio 48:52); ¹H NMR (400 MHz, (CD₃)₂SO): δ = 3.05–3.10 and 3.14–3.18 (1H, 2× m, ABX), 3.29–3.32 and 3.35–3.39 (1H, 2× m, ABX), 3.75 and 3.76 (3H, 2× s), 3.85–3.89 and 4.23–4.26 (1H, 2× m, ABX), 5.46 and 5.62 (1H, 2× s, CHAr), 6.89 and 6.93 (2H, 2× d, J = 8.6 Hz, ArH), 7.37 and 7.44 (2H, 2× d, J = 8.5 Hz, ArH).

4.1.2.2. 2-(4-Hydroxyphenyl)-1,3-thiazolidine-4-carboxylic acid (7b). Yield: 99% (8.9 g), white solid, mp 165–167 °C (lit. [16] 167–169 °C). The ¹H NMR spectrum showed the presence of the two diastereoisomers (2*R*,4*R*) and (2*S*,4*R*) (ratio 50:50); ¹H NMR (400 MHz, (CD₃)₂SO): δ = 3.02–3.07 and 3.13–3.17 (1H, 2× m, ABX), 3.25–3.28 and 3.34–3.37 (1H, 2× m, ABX), 3.82–3.86 and 4.24–4.26 (1H, 2× m, ABX), 5.40 and 5.54 (1H, 2× s, CHAr), 6.70 and 6.74 (2H, 2× d, J = 8.4 Hz, ArH), 7.25 and 7.31 (2H, 2× d, J = 8.1 Hz, ArH).

4.1.3. 5,5-Dimethyl-2-phenyl-1,3-thiazolidine-4-carboxylic acid (**10**)

A solution of benzaldehyde (0.54 g, 5.1 mmol) in methanol (7 mL) was slowly added to a solution of D-penicillamine (0.69 g, 4.6 mmol) in methanol (90 mL). After stirring overnight at room temperature the mixture was concentrated under reduced pressure and the residue was washed with diethyl ether to give a white solid (1.02 g, 93%). mp 160–162 °C. The ¹H NMR spectrum showed the presence of the two diastereoisomers (2*R*,4*S*) and (2*S*,4*S*) (ratio 38:62); Minor isomer: ¹H NMR (400 MHz, CD₃OD): δ = 1.49 (3H, s), 1.71 (3H, s), 3.95 (1H, s), 5.92 (1H, CHPh), 7.54–7.55 (5H, m, ArH); Major isomer: ¹H NMR (400 MHz, CD₃OD): δ = 1.46 (3H, s), 1.74 (3H, s), 3.82 (1H, s), 5.68 (1H, CHPh), 7.37–7.41 (5H, m).

4.1.4. General procedure for the synthesis of 1*H*,3*H*-pyrrolo[1,2-*c*]thiazole carboxylates **8** and **11**

A solution of the appropriate thiazolidine-4-carboxylic acid (12.0 mmol), dimethyl acetylenedicarboxylate (1.5 equiv., 18.0 mmol) and Ac₂O (40 mL) was heated at 110 °C during the 4 h. The reaction was cooled to room temperature and was diluted with CH₂Cl₂ (100 mL). The organic phase was washed with saturated aqueous solution of NaHCO₃ and with water, dried (Na₂SO₄) and the solvent evaporated off. The crude product was purified by flash chromatography [hexane-ethyl acetate].

4.1.4.1. Dimethyl (3*R*)-3-(4-methoxyphenyl)-5-methyl-1*H*,3*H*-pyrrolo[1,2-*c*]thiazole-6,7-dicarboxylate (8a**).** Purification by flash chromatography [hexane-ethyl acetate (2:1)] gave **8a** as a white solid (2.3 g, 52%); mp 80–82 °C (from diethyl ether); IR (KBr): ν_{max} = 1736, 1697, 1516, 1444, 1288, 1209, 1088 cm⁻¹; ¹H NMR (400 MHz, CDCl₃): δ = 2.00 (3H, s), 3.80 (3H, s), 3.83 (6H, s), 4.30 (1H, d, J = 14.9 Hz), 4.47 (1H, d, J = 14.9 Hz), 6.27 (1H, s), 6.86 (2H, d, J = 8.6 Hz), 7.02 (2H, d, J = 8.6 Hz); ¹³C NMR (100 MHz, CDCl₃): δ = 11.42, 29.98, 51.38, 51.56, 55.36, 64.87, 106.71, 114.59, 117.38, 127.23, 130.73, 131.93, 140.43, 160.08, 164.08, 165.36; HRMS (EI-TOF) *m/z* 361.0988 (M⁺, C₁₈H₁₉NO₅S requires 361.0984).

4.1.4.2. Dimethyl (3*R*)-3-(4-acetoxyphenyl)-5-methyl-1*H*,3*H*-pyrrolo[1,2-*c*]thiazole-6,7-dicarboxylate (8b**).** Purification by flash

chromatography [hexane-ethyl acetate (3:1), hexane-ethyl acetate (2:1), then hexane-ethyl acetate (1:1)] gave **8b** as a white solid (2.0 g, 42%); mp 90–92 °C (from ethyl acetate/hexane); IR (KBr): ν_{max} = 1766, 1734, 1709, 1437, 1367, 1296, 1215, 1095 cm⁻¹; ¹H NMR (400 MHz, CDCl₃): δ = 2.03 (3H, s), 2.26 (3H, s), 3.81 (6H, m), 4.29 (1H, d, J = 14.9 Hz), 4.44 (1H, d, J = 14.9 Hz), 6.32 (1H, s), 7.07 (4H, s, ArH); ¹³C NMR (100 MHz, CDCl₃): δ = 11.37, 20.97, 29.88, 51.29, 51.45, 64.23, 106.83, 117.36, 122.34, 126.84, 130.62, 137.59, 140.34, 150.90, 163.84, 165.10, 168.94; HRMS (EI-TOF) *m/z* 389.0935 (M⁺, C₁₉H₁₉NO₆S requires 389.0933).

4.1.4.3. Dimethyl (3*S*)-1,1,5-trimethyl-3-phenyl-1*H*,3*H*-pyrrolo[1,2-*c*]thiazole-6,7-dicarboxylate (11**).** Purification by flash chromatography [hexane-ethyl acetate (3:1), then hexane-ethyl acetate (2:1)] gave **7** as a yellowish oil (3.1 g, 73%); IR (KBr): ν_{max} = 1709, 1531, 1441, 1396, 1294, 1213, 1172 cm⁻¹; ¹H NMR (400 MHz, CDCl₃): δ = 1.84 (3H, s), 1.90 (3H, s), 1.95 (3H, s), 3.80 (3H, s), 3.84 (3H, s), 6.34 (1H, s, CHPh), 7.07–7.09 (2H, m, ArH), 7.31–7.36 (3H, m, ArH); ¹³C NMR (100 MHz, CDCl₃): δ = 11.26, 30.78, 31.92, 51.55, 51.58, 52.86, 64.17, 106.28, 117.67, 125.80, 128.79, 129.20, 129.21, 140.38, 145.73, 164.98, 165.50; HRMS (EI-TOF) *m/z* 359.1195 (M⁺, C₁₉H₂₁NO₄S requires 359.1191).

4.1.5. General procedure for the synthesis of 6,7-bis(hydroxymethyl)-1*H*,3*H*-pyrrolo[1,2-*c*]thiazole carboxylates **9** and **12**

A solution of the appropriate 5-methyl-1*H*,3*H*-pyrrolo[1,2-*c*]thiazole-carboxylate **8** or **11** (2.9 mmol) in dry dichloromethane (30 mL) was added dropwise to a suspension of lithium aluminum hydride (2.2 eq., 0.24 g, 6.4 mmol) in anhydrous diethyl ether (40 mL) at 0 °C. The solution was refluxed for 1.5 h after the addition was completed and then cooled on an ice bath. The excess of hydride was carefully decomposed by addition of ethyl acetate followed by slow addition of water (0.3 mL), NaOH 15% (0.3 mL) and water (0.9 mL). The mixture was filtered through celite and the inorganic residue was washed with several portions of hot dichloromethane. The filtrate was dried (Na₂SO₄) and the solvent evaporated off. The crude product was purified by flash chromatography [hexane-ethyl acetate] or recrystallization.

For the synthesis of compound **8b** 3.3 equivalents of lithium aluminum hydride (0.36 g, 9.6 mmol) were used. In this case the excess of hydride was eliminated by the addition of ethyl acetate followed by slow addition of water (0.4 mL), NaOH 15% (0.4 mL) and water (1.2 mL).

4.1.5.1. (3*R*)-6,7-Bis(hydroxymethyl)-3-(4-methoxyphenyl)-5-methyl-1*H*,3*H*-pyrrolo[1,2-*c*]thiazole (9a**).** Recrystallization with diethyl ether gave **9a** as a white solid (0.52 g, 58%); mp 119–121 °C; IR (KBr): ν_{max} = 3392, 1614, 1514, 1435, 1338, 1286, 1255, 1172, 1009 cm⁻¹; ¹H NMR (400 MHz, CDCl₃): δ = 1.84 (3H, s), 2.38 (1H, bs), 2.53 (1H, bs), 3.79 (3H, s), 4.08 (1H, d, J = 12.8 Hz), 4.28 (1H, d, J = 12.8 Hz), 4.48 (1H, d, J = 12.0 Hz), 4.53 (1H, d, J = 12.0 Hz), 4.59 (2H, s), 6.21 (1H, s, CHAr), 6.84 (2H, d, J = 8.4 Hz, ArH), 7.02 (2H, d, J = 8.4 Hz, ArH); ¹³C NMR (100 MHz, CDCl₃): δ = 9.96, 27.62, 55.33, 56.48, 56.79, 64.26, 113.30, 114.34, 123.09, 123.46, 127.25, 131.49, 133.38, 159.73; HRMS (EI-TOF) *m/z* 305.1085 (M⁺, C₁₆H₁₉NO₃S requires 305.1086); [α]_D²⁰ = + 230 (c 1, CH₂Cl₂).

4.1.5.2. (3*R*)-6,7-Bis(hydroxymethyl)-3-(4-hydroxyphenyl)-5-methyl-1*H*,3*H*-pyrrolo[1,2-*c*]thiazole (9b**).** Recrystallization with diethyl ether gave **9b** as a pale brown solid (0.43 g, 52%); mp > 220 °C (with decomposition); IR (KBr): ν_{max} = 3263, 1612, 1518, 1427, 1363, 1277, 1240, 982 cm⁻¹; ¹H NMR (400 MHz, CD₃OD): δ = 1.84 (3H, s), 4.07 (1H, d, J = 13.1 Hz), 4.29 (1H, d, J = 13.1 Hz), 4.43 (2H, s), 4.52 (1H, d, J = 12.1 Hz), 4.56 (1H, d, J = 12.1 Hz), 6.30

(1H, s, CHAr), 6.71 (2H, d, $J = 8.4$ Hz, ArH), 6.92 (2H, d, $J = 8.4$ Hz, ArH); ^{13}C NMR (100 MHz, CD_3OD): $\delta = 9.94, 28.12, 56.16, 56.62, 65.24, 114.13, 116.45, 124.06, 124.32, 128.47, 132.93, 134.34, 158.72$; HRMS (ESI-TOF) m/z 314.0829 ($[\text{M} + \text{Na}]^+$, $\text{C}_{15}\text{H}_{17}\text{NO}_3\text{SNa}$ requires 314.0821); $[\alpha]_{\text{D}}^{20} = +245$ (c 1, MeOH).

4.1.5.3. (3*S*)-6,7-Bis(hydroxymethyl)-1,1,5-trimethyl-3-phenyl-1*H*,3*H*-pyrrolo[1,2-*c*]thiazole (**12**). Purification by flash chromatography [hexane-ethyl acetate (1:2), then hexane-ethyl acetate (1:4)] gave **12** as a colorless oil (0.45 g, 51%); IR (film): $\nu_{\text{max}} = 3375, 1537, 1456, 1433, 1402, 1363, 1120, 989\text{ cm}^{-1}$; ^1H NMR (400 MHz, CDCl_3): $\delta = 1.78$ (3H, s), 1.83 (3H, s), 1.85 (3H, s), 4.49 (1H, d, $J = 12.1$ Hz, CH_2), 4.53 (1H, d, $J = 12.1$ Hz, CH_2), 4.65 (2H, s, CH_2), 6.30 (1H, s, CHPh), 7.06–7.09 (2H, m, ArH), 7.29–7.32 (3H, m, ArH); ^{13}C NMR (100 MHz, CDCl_3): $\delta = 9.87, 32.64, 33.82, 52.00, 55.28, 56.27, 64.04, 111.90, 121.86, 123.90, 125.91, 128.36, 128.96, 140.00, 141.82$; HRMS (EI-TOF) m/z 303.1295 (M^+ , $\text{C}_{17}\text{H}_{21}\text{NO}_2\text{S}$ requires 303.1293); $[\alpha]_{\text{D}}^{20} = -205$ (c 1, CH_2Cl_2).

4.2. Biological evaluation

4.2.1. Cell culture

Human breast carcinoma cell lines HCC1954 and HCC1806 were cultured in RPMI-1640 medium (Sigma Aldrich®, EUA) supplemented with 10% and 5% of fetal bovine serum (FBS) (Sigma Aldrich®, EUA), respectively, 2.5 g L^{-1} of D-(+)-glucose (Sigma Aldrich®, EUA), 400 mM of sodium pyruvate (Gibco®, UK), 100 U mL^{-1} of penicillin and 100 U mL^{-1} of streptomycin (Gibco®, UK), under an atmosphere containing 5% CO_2 at 37°C . Human breast adenocarcinoma cell line MCF7 was cultured in DMEM (Sigma Aldrich®, EUA) supplemented with 10% of FBS, 100 mM of sodium pyruvate, 100 U mL^{-1} of penicillin and 100 U mL^{-1} of streptomycin, under an atmosphere containing 5% CO_2 at 37°C .

4.2.2. Cytotoxicity

The cells were plated in 96-well culture plates at a density of 2×10^4 cells per well and incubated overnight to allow cell attachment. All compounds were dissolved in dimethylsulphoxide (DMSO, Sigma Aldrich®, EUA) at various concentrations and diluted in culture media. Cells were then incubated with the compounds for 24, 48, 72 and 96 h. The metabolic activity was determined by MTT assay [17,18] (3-(4,5-dimethylthiazol-2-yl)-2,5-diphenyl tetrazolium bromide; MTT, Sigma Aldrich®, EUA). Briefly, cell culture were washed with phosphate saline buffer (PBS: 137 mM NaCl, 2.7 mM KCl, 10 mM $\text{Na}_2\text{HPO}_4 \cdot 2\text{H}_2\text{O}$, 2.0 mM KH_2PO_4 ; pH = 7.4) and incubated with 0.5 mg mL^{-1} MTT (Sigma Aldrich®, EUA), pH = 7.4, at 37°C for 4 h. Then, formazan crystals were dissolved in acid isopropanol (0.04 M 37% hydrochloric acid in isopropanol; Sigma Aldrich®, EUA). The results allowed to establish dose–response curves and to calculate IC_{50} values, the concentration required to inhibit cell proliferation by 50%.

4.2.3. Clonogenic assay

For the clonogenic assay cells were plated in 6-well culture plates at a density of 5×10^5 cells per well and incubated to allow cell attachment. Incubation with the IC_{50} of **3** or **9b** was made for 48 h. Cells were harvested, counted and 1000, 3000 or 5000 cells were plated. After 12 days, cells were fixed with methanol, stained with crystal violet and individual colonies were counted.

4.2.4. Sulphorhodamine B assay

For total protein production evaluation, cells were plated in 24-well culture plates at a density of 4×10^4 cells per well and incubated overnight to allow cell attachment. Cell cultures were incubated with IC_{50} concentrations of the compounds **3** and **9b** for 48 h

(final DMSO concentration 1%). SRB assay was performed as described [19]. Briefly, cells were washed with ultra-pure water and twice with PBS. Cells were then incubated with 1% acetic acid in methanol for 30 min prior to incubation with 0.4% SRB (Sigma Aldrich®, EUA) dissolved in 1% acetic acid (Sigma Aldrich®, EUA) in methanol (Sigma Aldrich®, EUA) for 1 h in the dark. After incubation SRB crystals were dissolved in 10 mM Tris–NaOH, pH 10.

4.2.5. Cell viability and types of cell death

For analysis of cell viability and types of cell death, 2×10^6 cells were incubated overnight to allow attachment and then were treated with IC_{50} of **3** or **9b** for 48 h (final DMSO concentration 0.1%). Then, cells were collected, centrifuged and washed with PBS prior to incubation with binding buffer, $2.5\text{ }\mu\text{L}$ An-V–FITC and $1\text{ }\mu\text{L}$ propidium iodide (kit Immunotech) for 15 min, at 4°C in the dark. $400\text{ }\mu\text{L}$ PBS were added and samples were analyzed in a FACSCalibur cytometer (BD Biosciences, EUA). Excitation was set at 488 nm, and the emission filters were set at for An-V–FITC and propidium iodide, respectively.

4.2.6. P53 expression

Western Blot was used to evaluate the expression of p53 protein. Cells were treated with the IC_{50} of **3** or **9b** during 48 h. Total protein extracts were prepared on ice using a solution of radioimmuno precipitation assay (RIPA) buffer supplemented with cComplete Mini (Roche). After sonication and centrifugation at 14,000 g, the samples were kept at -80°C prior use. Protein content was determined by bicinchoninic (BCA) method. Sodium dodecyl sulfate polyacrylamide gel electrophoresis (SDS–PAGE) was held using a 10% acrylamide gel for 20 min at 80 V followed by 160 V till 1 h 10 min. Subsequently proteins were electrotransferred to nitrocellulose (PVDF) membranes at 100 V during 1 h. Blocking of PVDF membranes was performed with 4% bovine serum albumin (BSA) in tris-buffered saline tween-20 (TBS-T) for 1 h at room temperature with stirring. Incubation with primary antibodies, Actin (Sigma–Aldrich) and p53 (mouse anti-human p53-DO7, Santa Cruz Biotechnology, Inc.) was performed overnight at 4°C . After several washes with TBS-T, membranes were incubated with secondary antibody (anti-mouse antibody) for 1 h at room temperature. New washes were performed and ultimately the blots were stained with fluorescent reagent elemental chlorine free (ECF) and reading was performed in 9000 Typhoon FLA equipment. Quantification of fluorescence was performed using the ImageQuant Software (GE Healthcare).

4.2.7. Bax/Bcl-2 analysis

Bax and Bcl-2 expression was also analyzed by flow cytometry using monoclonal antibodies conjugated with phycoerythrin (PE) and FITC respectively. Briefly, 2×10^6 cells were incubated overnight to allow cell attachment and were treated with IC_{50} of **3** or **9b** for 48 h (DMSO 0.1%). Cells were collected, centrifuged and washed with PBS prior to incubation with permeabilizing solution (Intracell Kit, Immunostep), $3\text{ }\mu\text{L}$ Bax–PE (Santa Cruz Biotechnology, Inc.) and $3\text{ }\mu\text{L}$ Bcl-2–FITC (Santa Cruz Biotechnology, Inc.), for 15 min in the dark. After washing with PBS, analysis was performed in the FACSCalibur cytometer with excitation at 488 nm, and emission filter at 530/30 and 585/42 for Bcl-2 and Bax, respectively.

4.2.8. Cell cycle analysis

For analysis of DNA content, 2×10^6 cells were incubated overnight to allow cell attachment and then were treated with IC_{50} of **3** or **9b** for 48 h (DMSO 0.1%). Cells were collected, centrifuged, and fixed with ice-cold ethanol (70%) for 30 min in the dark. Then, cells were washed with PBS and incubated with PI/RNase solution (Immunostep) for 15 min RT. Cells were analyzed in the

FACSCalibur cytometer with an excitation wavelength of 488 nm, and emission filter at of 585/42.

4.2.9. Comet assay

Damage in cell DNA was analyzed with alkaline single-cell gel electrophoresis, comet assay [20]. Briefly, 5×10^5 cells were treated with IC_{50} of **3** or **9b** and with the triple of the first value (DMSO 0.1% for both cases) for 48 h. Positive control was prepared from negative control with administration of 20 nM of hydroxide peroxide (Sigma Aldrich®, EUA) for 15 min at -4°C . Controls and treated cells were then collected and counted in order to prepare a suspension with 5×10^4 g mL $^{-1}$. Cells suspensions were diluted 1:1 in 1% low melting point agarose and applied in Starfrost slides previously overlaid with 1% normal melting point agarose. The slides were submerged in alkaline lysis solution (2.5 M NaCl, 100 mM EDTA, 10 mM Tris, 10% DMSO and 1% Triton x-100, Sigma Aldrich®, EUA) overnight. Slides were equilibrated in alkaline electrophoresis buffer (300 mM NaOH and 1 mM EDTA, pH > 13) and then were submitted to a potential difference of 25 V and current of 1 A, for 15 min. After electrophoresis, slides were incubated in neutralizing buffer (0.4 M Tris, pH 7.4) 3 times, 5 min each, and stained with 25 $\mu\text{g mL}^{-1}$ ethidium bromide for 20 min. Slides were washed in distilled water and visualized in a fluorescent inverted microscope Motic with excitation at 546 nm with a 100 W mercury lamp with emission at 580/10. Image acquisition was performed in Motic Images 2.0 (Microscope world, EUA).

Acknowledgments

Thanks are due to FCT (Project PEst-OE/QUI/UI0313/2014, SFRH/BD/44957/2008 PhD Grant received by M. Laranjo, SFRH/BD/61378/2009 PhD Grant received by A. F. Brito), for financial support. We acknowledge the Nuclear Magnetic Resonance Laboratory of the Coimbra Chemistry Center (www.nmrccc.uc.pt), University of Coimbra for obtaining the NMR data.

Appendix A. Supplementary data

Supplementary data related to this article can be found at <http://dx.doi.org/10.1016/j.ejmech.2014.04.008>.

References

- [1] A. Jemal, F. Bray, M.M. Center, J. Ferlay, E. Ward, D. Forman, Global cancer statistics, CA: a Cancer Journal for Clinicians 61 (2011) 69–90.
- [2] N. Turner, A. Tutt, A. Ashworth, Hallmarks of 'BRCAness' in sporadic cancers, Nature Reviews Cancer 4 (2004) 814–819.
- [3] E. Amir, B. Seruga, R. Serrano, A. Ocana, Targeting DNA repair in breast cancer: a clinical and translational update, Cancer Treatment Reviews 36 (2010) 557–565.
- [4] M.L.L. Soares, A.F. Brito, M. Laranjo, A.M. Abrantes, M.F. Botelho, J.A. Paixão, A.M. Beja, M.R. Silva, T.M.V.D. Pinho e Melo, Chiral 6-hydroxymethyl-1H,3H-pyrrolo[1,2-c]thiazoles: novel antitumor DNA monoalkylating agents, European Journal of Medicinal Chemistry 45 (2010) 4676–4681.
- [5] M.L.L. Soares, A.F. Brito, M. Laranjo, J.A. Paixão, M.F. Botelho, T.M.V.D. Pinho e Melo, Chiral 6,7-bis(hydroxymethyl)-1H,3H-pyrrolo[1,2-c]thiazoles with anti-breast cancer properties, European Journal of Medicinal Chemistry 60 (2013) 254–262.
- [6] M. Olivier, R. Eeles, M. Hollstein, M.A. Khan, C.C. Harris, P. Hainaut, The IARC TP53 database: new online mutation analysis and recommendations to users, Human Mutation 19 (2002) 607–614.
- [7] M. Lacroix, R.A. Toillon, G. Leclercq, p53 and breast cancer, an update, Endocrine-Related Cancer 13 (2006) 293–325.
- [8] R.J. Youle, A. Strasser, The BCL-2 protein family: opposing activities that mediate cell death, Nature Reviews Molecular Cell Biology 9 (2008) 47–59.
- [9] D. Ren, H.C. Tu, H. Kim, G.X. Wang, G.R. Bean, O. Takeuchi, J.R. Jeffers, G.P. Zambetti, J.J. Hsieh, E.H. Cheng, BID, BIM, and PUMA are essential for activation of the BAX- and BAK-dependent cell death program, Science 330 (2010) 1390–1393.
- [10] R.K. Sodhi, N. Singh, A.S. Jaggi, Poly(ADP-ribose) polymerase-1 (PARP-1) and its therapeutic implications, Vascular Pharmacology 53 (2010) 77–87.
- [11] J.A. Seiler, C. Conti, A. Syed, M.I. Aladjem, Y. Pommier, The intra-S-phase checkpoint affects both DNA replication initiation and elongation: single-cell and -DNA fiber analyses, Molecular and Cellular Biology 27 (2007) 5806–5818.
- [12] A. Poehlmann, A. Roessner, Importance of DNA damage checkpoints in the pathogenesis of human cancers, Pathology Research and Practice 206 (2010) 591–601.
- [13] C.E. Caldon, R.J. Daly, R.L. Sutherland, E.A. Musgrove, Cell cycle control in breast cancer cells, Journal of Cellular Biochemistry 97 (2006) 261–274.
- [14] P. Moller, The alkaline comet assay: towards validation in biomonitoring of DNA damaging exposures, Basic & Clinical Pharmacology & Toxicology 98 (2006) 336–345.
- [15] J.H. Wu, N.J. Jones, Assessment of DNA interstrand crosslinks using the modified alkaline comet assay, Methods in Molecular Biology 817 (2012) 165–181.
- [16] H. Soloway, F. Kipnis, J. Ornfelt, P.E. Spoerri, 2-Substituted-thiazolidine-4-carboxylic Acids, Journal of the American Chemical Society 70 (1948) 1667–1668.
- [17] L. Laranjo, A.L. Neves, T. Villanueva, J. Cruz, A.B. Sá, C. Sakellarides, Patients' access to their medical records, Acta Médica Portuguesa 26 (2013) 265–270.
- [18] T. Mosmann, Rapid colorimetric assay for cellular growth and survival: application to proliferation and cytotoxicity assays, Journal of Immunological Methods 65 (1983) 55–63.
- [19] V. Vichai, K. Kirtikara, Sulforhodamine B colorimetric assay for cytotoxicity screening, Nature Protocols 1 (2006) 1112–1116.
- [20] R.R. Tice, E. Agurell, D. Anderson, B. Burlinson, A. Hartmann, H. Kobayashi, Y. Miyamae, E. Rojas, J.C. Ryu, Y.F. Sasaki, Single cell gel/comet assay: guidelines for in vitro and in vivo genetic toxicology testing, Environmental and Molecular Mutagenesis 35 (2000) 206–221.